Neuro-Oncology

24(7), 1166–1175, 2022 | https://doi.org/10.1093/neuonc/noab284 | Advance Access date 11 December 2021

Revised clinical and molecular risk strata define the incidence and pattern of failure in medulloblastoma following risk-adapted radiotherapy and dose-intensive chemotherapy: results from a phase III multi-institutional study

John T. Lucas Jr.[†], Christopher L. Tinkle[†], Jie Huang, Arzu Onar-Thomas, Sudharsan Srinivasan, Parker Tumlin, Jared B. Becksfort, Paul Klimo, Frederick A. Boop, Giles W. Robinson, Brent A. Orr, Julie H. Harreld, Matthew J. Krasin, Paul A. Northcott, David W. Ellison, Amar Gajjar, and Thomas E. Merchant

Department of Radiation Oncology, St. Jude Children's Research Hospital, Memphis, Tennessee, USA (J.T.L., C.L.T., S.S., P.T., J.B., M.J.K., T.E.M.); Department of Biostatistics, St. Jude Children's Research Hospital, Memphis, Tennessee, USA (J.H., A.O-T.); Department of Surgery, St. Jude Children's Research Hospital, Memphis, Tennessee, USA (P.K., F.A.B.); Department of Oncology, St. Jude Children's Research Hospital, Memphis, Tennessee, USA (G.W.R., A.G.); Department of Pathology, St. Jude Children's Research Hospital, Memphis, Tennessee, USA (B.A.O., D.W.E.); Department of Diagnostic Imaging, St. Jude Children's Research Hospital, Memphis, Tennessee, USA (J.H.H.); Department of Developmental Neurobiology, St. Jude Children's Research Hospital, Memphis, Tennessee, USA (P.A.N.)

Present affiliation: University of Michigan, Ann Arbor, Michigan, USA (S.S.); West Virginia University, Morgantown, West Virginia, 26506, USA (P.T.)

Corresponding Authors: John T. Lucas Jr., MD, MS, Department of Radiation Oncology, St. Jude Children's Research Hospital, 262 Danny Thomas Place, MS 210, Memphis, TN 38105-3678, USA (john.lucas@stjude.org); Christopher L. Tinkle, MD, PhD, Department of Radiation Oncology, St. Jude Children's Research Hospital, 262 Danny Thomas Place, MS 210, Memphis, TN 38105-3678, USA (christopher.tinkle@stjude.org).

[†]These authors contributed equally to this work.

Abstract

Background. We characterize the patterns of progression across medulloblastoma (MB) clinical risk and molecular subgroups from SJMB03, a Phase III clinical trial.

Methods. One hundred and fifty-five pediatric patients with newly diagnosed MB were treated on a prospective, multi-center phase III trial of adjuvant radiotherapy (RT) and dose-intense chemotherapy with autologous stem cell transplant. Craniospinal radiotherapy to 23.4 Gy (average risk, AR) or 36-39.6 Gy (high risk, HR) was followed by conformal RT with a 1 cm clinical target volume to a cumulative dose of 55.8 Gy. Subgroup was determined using 450K DNA methylation. Progression was classified anatomically (primary site failure (PSF) +/– distant failure (DF), or isolated DF), and dosimetrically.

Results. Thirty-two patients have progressed (median follow-up 11.0 years (range, 0.3–16.5 y) for patients without progression). Anatomic failure pattern differed by clinical risk ($P = .0054$) and methylation subgroup ($P = .0034$). The 5-year cumulative incidence (CI) of PSF was 5.1% and 5.6% in AR and HR patients, respectively ($P = .92$), and did not differ across subgroups ($P = .15$). 5-year CI of DF was 7.1% vs. 28.1% for AR vs. HR ($P = .0003$); and 0% for WNT,

15.3% for SHH, 32.9% for G3, and 9.7% for G4 ($P = .0024$). Of 9 patients with PSF, 8 were within the primary site RT field and 4 represented SHH tumors.

Conclusions. The low incidence of PSF following conformal primary site RT is comparable to prior studies using larger primary site or posterior fossa boost volumes. Distinct anatomic failure patterns across MB subgroups suggest subgroup-specific treatment strategies should be considered.

Key Points

- Reduced target margins do not compromise local control.
- Clinical and molecular risk stratification identifies patients with increased risk of local failure who may benefit from alternative local control strategies.

Importance of the Study

The use of reduced target margins does not increase in primary site failure. These results support the practice of reduced target margins to lower overall dose to eloquent structure of the brain. High molecular and clinical risk SHH tumors fail both at the primary site and distantly while high molecular risk group 3 and 4 patients fail predominately at distant areas within the CNS. Differences in disease distribution highlight regions at reduced risk of treatment failure which may be considered for radiation avoidance to limit morbidity in future trials. Revised clinical and molecular risk stratification successfully identifies patients who may benefit from alternative therapeutic strategies.

Medulloblastoma is the most common malignant pediatric brain tumor, accounting for the majority of CNS embryonal tumors.[1] Due to the propensity for leptomeningeal spread, the most commonly employed treatment paradigm for children older than 3 years of age includes maximal safe tumor resection, radiation therapy (RT) encompassing the entire neuraxis followed by primary site "boost" radiation, and multi-agent chemotherapy. With this approach, 5-year survival rates have improved to approximately 75–85% for patients at average-risk of relapse (i.e., patients lacking significant residual or metastatic disease) and 60–70% for those at high-risk.[2,3] It is now well understood that, despite the critical role of craniospinal irradiation,[4,5] the benefit provided by this therapy is counterbalanced by its profound toxicities, including lifelong deficits in neurocognition, hearing, and endocrine function, as well as increased risk for second malignancies and vascular injury.[6–9] Consequently, RT has been the most studied intervention within clinical trials for medulloblastoma, with investigations exploring the omission and/or delay of RT, reductions of RT field size and/or dose, sequencing of RT, and radiation quality.

Following initial pilot studies demonstrating the feasibility of reduced primary tumor site boost volume from the traditional entire posterior fossa to the more limited postoperative surgical bed following CSI,[10,11] Merchant and colleagues demonstrated a cumulative posterior fossa failure rate of 4.9% in average-risk patients treated with risk-adapted CSI to 23.4 Gy followed by entire posterior fossa boost to 36 Gy and primary tumor site irradiation to 55.8 Gy employing a 2-cm clinical target volume (CTV) on the prospective phase II SJMB96 clinical trial.[12] Patients with High-Risk (HR) were treated with 36 Gy CSI followed by primary site irradiation using the same CTV margin. After this, the Children's Oncology Group (COG) launched two, phase III, clinical trials for medulloblastoma, ACNS0331 and ACNS0332.[13,14] Recently published results from ACNS0331, in which average-risk patients aged 3 to 7 years were randomized to 23.4 Gy vs. 18 Gy of CSI and all patients were randomized to boost RT to the entire posterior fossa vs. the primary tumor site with a 1.5-cm CTV margin, demonstrated no significant differences in event-free survival or overall survival by primary tumor boost volume, although an increased risk for subsequent treatment failures was noted in the 18 Gy CSI arm.[15] RT guidelines for the recently closed ACNS00332 trial,[16] which addressed the potential radiosensitizing effect of adding carboplatin to vincristine concurrently with radiation in HR patients, included high-dose CSI followed by entire posterior fossa boost irradiation.[17] In parallel, the multi-institutional phase III clinical trial SJMB03 was initiated in 2003[13] (Supplementary Figure 1). In this study, two important modifications to RT guidelines from the preceding SJMB96 study were tested. First, the intermediate step of additional treatment of the posterior fossa after the initial CSI phase was dropped in AR patients, and second, the primary tumor CTV for both risk strata was further limited to a 1.0-cm margin.

Based largely on DNA methylation profiling, medulloblastoma is now known to be a heterogeneous disease comprising four distinct molecular subgroups (WNT, SHH, G3, and G4) with diverse clinical characteristics, genetic drivers of disease, and prognoses.[18,19] In addition, more detailed studies are showing these subgroups can be divided into 13 subtypes. The emergence of this critical heterogeneity has redoubled efforts to better define the optimal role of CSI and primary and metastatic site irradiation within and across the disease. While retrospective data from heterogeneously treated patient cohorts suggest differential

patterns of progression by molecular subgroup,[20] prospective data with detailed treatment information and associated radiation dosimetry are limited. The primary objective of this study was to evaluate the incidence of posterior fossa failure in patients treated on SJMB03. The dosimetric analysis was limited to patients treated at St. Jude Children's Research Hospital (St. Jude). Secondary objectives include evaluating the impact of clinical risk stratification and molecular subgroups on the pattern of treatment failure and the effect of reduced target margins employed on SJMB03, and the dose distribution to critical brain subregions.

Methods and Materials

Study Design and Patient Cohort

SJMB03 (NCT00085202) was a multi-institutional, phase III study of risk-adapted RT and dose-intensive chemotherapy with autologous stem cell rescue in patients aged 3–21 years (range, 5.4–11.9 years) with newly diagnosed medulloblastoma, supratentorial primitive neuroectodermal tumor, or atypical teratoid rhabdoid tumor.[13] Between September 9, 2003 and March 7, 2013, 330 eligible patients with medulloblastoma (MB) were enrolled, 155 of which were treated at St. Jude (100 average-risk [AR] and 55 high-risk patients [HR]). SJMB03 was approved by each site's Institutional Review Board with written, informed consent obtained from all patients and families.

Treatment Strategy

Patients were enrolled on SJMB03 after maximal safe surgical resection (Supplementary Figure 1). Baseline evaluations of the brain and spine included MRI as well as cerebrospinal fluid cytology. Gross total resection (GTR) or near total resection (NTR) was defined on postoperative imaging as either no remaining tumor or <1.5 cm^2 residual tumor, respectively, whereas subtotal resection (STR) was defined as >1.5cm^2 residual tumor. Repeat surgery was allowed prior to radiation and patients were stratified according to the maximum extent of resection from the last surgery and metastatic status. Average Risk (AR) MB criteria included 1) GTR/NTR, and 2) no radiographic, or cytologic evidence of CNS, or extra-neural dissemination. High risk (HR) criteria included 1) the presence of metastatic disease within the neuraxis, or 2) STR.

Risk-adapted photon radiotherapy consisted of 23.4 Gy CSI for AR patients or 36–36.9 Gy CSI for HR patients, followed by primary site irradiation to 55.8 Gy delivered in conventional 1.8 Gy fractions using conformal techniques. HR patients without metastatic disease or those with positive CSF cytology received 36 Gy CSI, while those with distant intracranial or spinal metastasis received 36–39.6 Gy CSI. Intracranial metastatic disease was treated to a cumulative dose of 54–55.8 Gy, while bulky spinal metastatic disease was treated to 50.4 Gy; metastatic site irradiation was delivered at the time of primary site RT following CSI. CSI was administered within 31 days of definitive surgery. Target volumes included a gross tumor volume (GTV), a 1.0 cm anatomically constrained isotropic CTV, and a 0.5 cm planning target volume (PTV) for the primary site and a metastatic target volume (MTV) and 0.5 cm PTV for overt metastatic disease >5 mm in maximal diameter. The GTV included all gross residual tumor and/or the contracted or collapsed resection cavity as determined from the initial preoperative MRI that defined the initially involved tissues and the postoperative MRI that identified any residual disease and delineated the resection cavity. Intensity-modulated RT was used for volume-based treatment plans of the primary site. Chemotherapy was initiated 6 weeks after completion of RT and consisted of four cycles of high-dose chemotherapy consisting of vincristine (1.0 mg/m^2 once daily [max dose 2.0 mg] on day 24 and 6), cisplatin (75 mg/m^2 once daily on day 24), and cyclophosphamide (2 g/m^2 once daily on days 23 and 22) with 4 weeks per cycle and each cycle being followed by autologous peripheral blood stem cell support on day 0.

Genome-Wide DNA Methylation Profiling and Next-Generation Sequencing

DNA and RNA were extracted from formalin-fixed paraffin-embedded or fresh-frozen tumor samples. Genome-wide DNA methylation profiling was performed on 155 patients using the Infinium Methylation EPIC BeadChip array as described previously, comprising our molecular cohort.[21,22] Methylation classification failed in 11 patients. Epigenomic classification was conducted on the molecular cohort, together with reference profiles obtained from a published brain tumor dataset and using the Molecular Neuropathology (MNP) brain tumor classifier (www.molecularneuropathology.org).[23] Ten patients had inconclusive classification scores and are excluded from methylation subgroup analyses. A revised clinical and molecular risk classification was utilized to review clinical events and is described in Gajjar *et al.*[24] Briefly, SHH high-risk patients were defined by the presence of TP53 mutation, LC/A histology, MYCN amplification, GLI2 amplification, and chromosome 17p loss. Group 3 and 4 patients could be classified as low-risk (M0 and subtype VII), intermediate-risk (M0 and subtype not within III or VII), or high-risk (M+ or subtype III or MYC amplified).

Patterns of Failure Evaluation

Cumulative radiotherapy dose profiles including CSI, primary site RT, and where applicable, metastatic site RT, were generated on the initial CSI CT simulation scan through co-registration of the of the boost site(s) CT simulation scan(s) (Supplementary Figure 2). Treatment failure volumes were manually delineated based on the diagnostic MRI(s) at the time of failure. Normal brain regions were delineated using FreeSurfer on the postoperative MRI (Supplementary Figure 3) (https://surfer.nmr.mgh.harvard.edu/fswiki/FreeSurferWiki). Trial defined primary site and metastatic disease volumes, all failure volumes, and normal brain regions were co-registered to the dose-accumulated CSI CT simulation scan and deformed to an MNI brain atlas.[25] Corresponding dosimetry and volumetric frequency maps of regions involved at diagnosis and failure were delineated. Treatment failures were classified according to their location (IV^{th} ventricle, cerebellar hemisphere, cerebellar pontine angle, or distant) and

imaging appearance (infiltrative, nodular, laminar).[26,27] Each failure was then assessed for its relationship to the treatment planning volumes (GTV, CTV, PTV), radiation dose profile (central, in-field, marginal, distant),[28–30] and overlap with normal brain structures. Briefly, central and in-field failures were defined as a treatment failure volume that was completely encompassed either by the 95% or 80% prescription isodose line, respectively.

Statistical Analysis

Competing risk analysis was conducted using PSF or DF as the outcome variable. The following events were considered as competing risks: failure of the other type, secondary malignancy, or death without prior failure. Per this definition, one patient who experienced second malignancy prior to disease progression was counted as having a competing event in the competing risk analysis. The cumulative incidence functions of PSF and distant failure since date of diagnosis were calculated using Gray's method. Fisher's exact test was used to investigate associations between categorical variables. Statistical analyses were performed using SAS -9.4 (Cary, NC).

Results

Demographics, Clinical Characteristics, and Risk Stratification

Of 155 patients, 100 (64.5%) were AR, and 55 (35.5%) were HR (Table 1). Eight (5%) were metastatic by cytology (M1) while 46 (29.7%) were metastatic due to the presence of disseminated disease by imaging (M2/M3). A GTR was achieved in 147 (94.8%) patients and a Subtotal Resection (STR) in 8 (5.2%). Patients were stratified into AR or HR arms (Table 1). Large cell anaplasia was present in 13 (16.8%) of patients, while 114 (73.5%) had classic histology. Methylation group was WNT, SHH, Group 3, Group 4, and unknown in 14.2%, 17.4%, 20.6%, 40.6%, and 7.1% of patients.

Table 1. Patient and Disease Characteristics

Patient Characteristics	Average Risk ($n = 100$)		High Risk ($n = 55$)	
	n	%	*n*	%
Age (years median IQR)	9.0 (6.7, 11.9)		7.2 (5.4, 9.7)	
Sex				
Male	67	67.0	32	58.2
Female	33	33.0	23	41.8
Disease extent				
M0	100	100.0	1	1.8
M1	0	0	8	14.5
M2	0	0	15	27.3
M3	0	0	31	56.4
Extent of resection				
STR	0	0	8	14.5
GTR/NTR	100	100.0	47	85.5
Histology				
Classic	74	74.0	40	72.7
Large cell anaplasia	13	13.0	13	23.6
Other	13	13.0	2	3.6
Subgroup				
WNT	19	19.0	3	5.5
SHH	20	20.0	7	12.7
Group 3	16	16.0	16	29.1
Group 4	38	38.0	25	45.5
Unknown	7	7.0	4	7.3

IQR: interquartile range, n: number, SHH: sonic hedgehog, M: metastasis, NTR: near total resection, GTR: gross total resection, STR: subtotal resection, NTR: near total resection, GTR: gross total resection, n: number, SHH: sonic hedgehog, M: metastasis.

Primary Site and Distant Failure by Clinical Risk Group and Molecular Subgroup

With a median follow-up of 11.0 years (range, 0.3–16.5 years) for patients who remain at risk, 32 patients have experienced treatment failure although one patient had second malignancy prior to disease progression. Data for the remaining 31 patients are shown in Figure 1A. The overall 5-year cumulative incidence of primary site failure was 5.1% (95% CI, 1.9–10.8%) and 5.6% (95% CI, 1.5–14.2%) in the average-risk ($n = 6$ of 100) and high-risk strata ($n = 3$ of 55) ($P = .92$) (Figure 1B, Supplementary Figure 6A and B). The 5-year cumulative incidence of distant failure was 7.1% (95% CI, 3.1–13.4%) and 28% (95% CI, 16.8–40.6%) in the average and high-risk group ($P = .0003$) (Figure 1C, Supplementary Figure 6C and D).

The 5-year cumulative incidence of primary site failure was 0%, 15.3% (95% CI 4.6–31.7%), 6.7% (95% CI 1.1–19.6%), and 3.2% (95% CI 5.9–10.0%) in the WNT, SHH, Group 3, and Group 4 subgroup ($P = .15$) (Figure 1D). When comparing SHH ($n = 27$) vs. others (combined Group 3/Group 4/WNT, $n = 117$), we observed a significant increase in the cumulative incidence of primary site failure in the SHH subgroup (Gray's test P-value = .0358) (Figure 1D). The 5-year cumulative incidence of distant failure was 0%, 15.3%, 32.9%, 9.7% and in the WNT, SHH, Group 3, Group 4 and subgroup ($P = .0024$) (Figure 1E).

Primary Site Imaging Characteristics at Diagnosis and Failure

The extent and localization of the primary tumor varied by methylation subgroup at diagnosis with SHH patients tending to be more hemispheric while Group 3 and Group 4 cases frequently extended craniocaudally and were predominately confined in and around the fourth ventricle (Figure 2). Of the nine cases of primary site failure, the imaging appearance included a nodular (9/9), cystic component (2/9), subependymal (2/9) and leptomeningeal (2/9) component. All but three of these failures occurred within the fourth ventricle (Table 2).

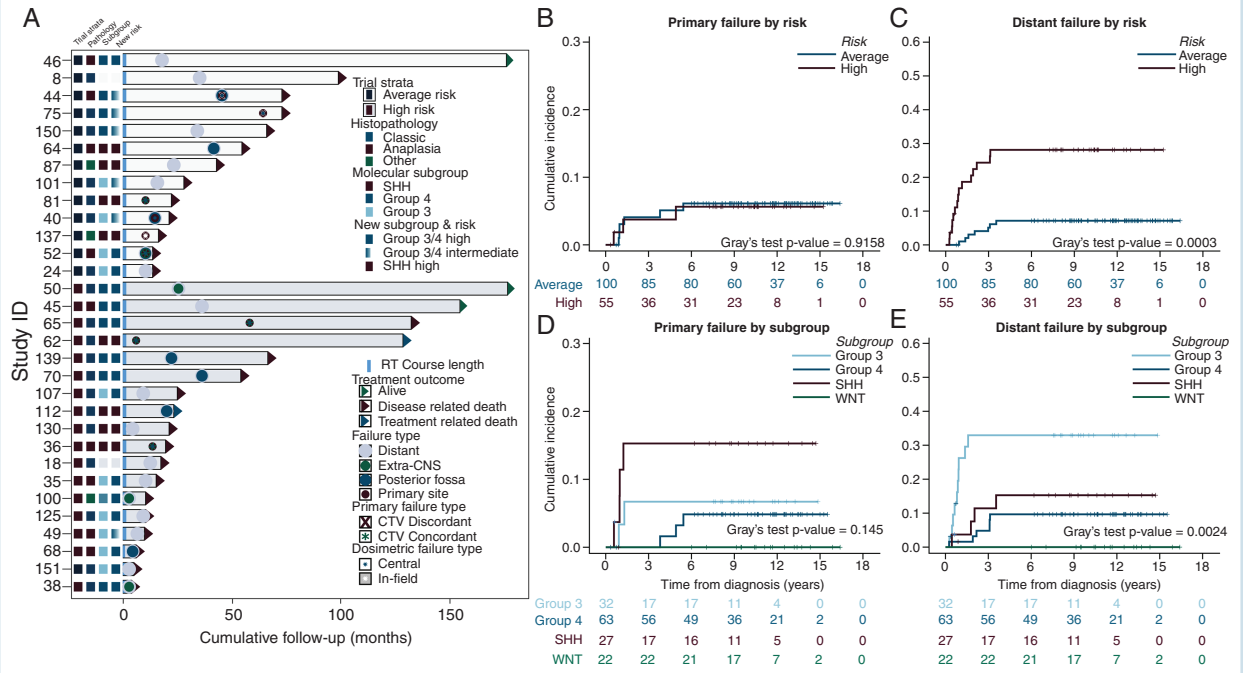

Fig. 1 Swimmer plot and cumulative incidence of primary site and distant failure by clinical risk and methylation group. A. Swimmer plot detailing the timeline of treatment, failure, and overall outcome for each patient by trial strata. Each failure event is detailed as to the corresponding type (i.e. distant, extra-CNS, posterior fossa and primary site failure). Primary site failures are also described according to the relation of the failure event and the delineated treatment volume (CTV) and corresponding radiation dosimetric coverage. B. Cumulative incidence of primary site failure stratified by risk category. C. Cumulative incidence of distance failure stratified by risk category. D. Cumulative incidence of primary site failure by subgroup. E. Cumulative incidence of distant failure by subgroup. ID: Patient Identify number, SHH: sonic hedgehog, RT: radiotherapy, CNS: central nervous system, CTV: clinical target volume.

Analysis of Primary Site Failures According to Targeting and Prescription Coverage

Primary site treatment failure volumes were evaluated according to the initial delineated CTV volume (Figure 1A, Supplementary Figure 4). Two cases showed >45% non-union (47.3% outside pCTV, and 67.1% outside pCTV) with the initial clinical target volume. Despite the CTV discordance in these cases, the reduced conformality of photon target volumes still resulted in the classification of each failure as central and in-field, respectively, relative to the 95% isodose line. All primary site failures were central with respect to their position relative to the 95% isodose line.

Analysis of Metastatic Site Failures According to Location

All metastatic site failures were delineated volumetrically on the failure brain MRI and deformed to an MNI brain atlas for comparison across subjects (Figure 2A, Supplementary Figure 5). Group 3 patients failed in the supratentorial brain and third ventricle more commonly than SHH, and Group 4 patients (Supplementary Figure 5B). While most metastatic site failures approximated the cerebellum beyond the primary site in the form of leptomeningeal seeding or nodular metastases, mass like supratentorial lesions were not infrequent. In initially M0 patients who experienced distant failure, we evaluated the frequency of normal brain regions involved by metastatic disease at the time of failure to better evaluate the potential for future region avoidance strategies. Potential areas of interest such as the hippocampus and hypothalamus were involved in 15% and 18% of patients, respectively (Supplementary Figure 5B and C).

Failure Status by Novel Risk Grouping

Prior analyses of the entire study cohort identified three low-risk groups (WNT, low-risk SHH, and low-risk combined group 3 and 4) with excellent progression-free survival and two very high-risk groups (high-risk SHH, high-risk combined group 3 and 4) with poor progression-free survival.[13,30] To that end, we evaluated PSF (Figure 2B) by this revised risk stratification (Supplementary Table 1, Figure 3). Figure 3A and B shows the cumulative incidence of local failure by the revised risk stratification. The SHH high subset had a 5-year cumulative incidence of local failure of 28% (95% CI 8.0–53.2%), while the Group 3 and Group 4 high and intermediate strata were 4.6% (95% CI 0.8–13.8%) and 6.9% (95% 1.2–20.2%), respectively. Most primary site and posterior fossa failures occurred in the SHH high group and the Group 3 and 4 intermediate or high-risk group (Figure 2B, Figure 3A and B, Supplementary Figure 6A, B, and E). The impact of surgical extent on local failure was not significant in the context of the revised stratification, although

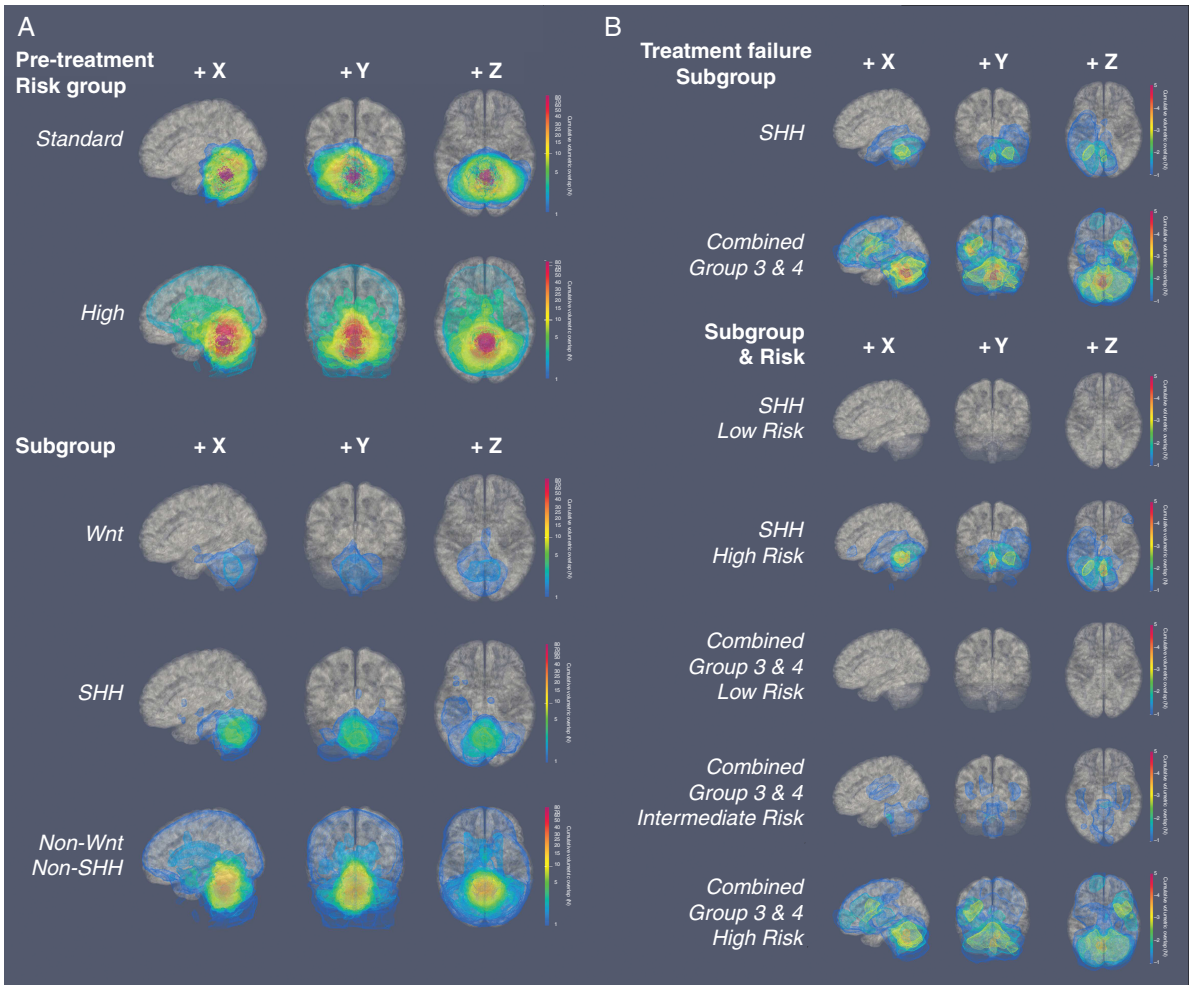

Fig. 2 Pretreatment and failure disease distribution by risk, molecular subgroup, and revised risk stratification. Probabilistic disease distributions are shown on sagittal, coronal and axial projections of a patient neutral MNI brain atlas at diagnosis and relapse. A. Pretreatment disease volumes are shown as a stratified by clinical risk group and molecular subgroup. B. Treatment failure disease volumes are shown as stratified by molecular subgroup, and the revised risk stratification proposed by Gajjar et al.[24].

the low rate of subtotal resections precluded assessment (Supplementary Figure 6G and H).

Discussion

The radiotherapy paradigm for medulloblastoma has evolved out of necessity over the course of the last three decades. The long-term morbidity associated with craniospinal radiotherapy has prompted investigators to consider a range of approaches including patient selection, dose de-escalation, field reduction, and alternative radiotherapy quality metrics to lessen the burden of cognitive, endocrine, hearing, and subsequent malignancies on childhood cancer survivors. SJMB03 evaluated the use of reduced target margins for the primary site regardless of clinical risk in medulloblastoma patients ages 3–21. In the interim, substantial advances in our understanding of the biology of the disease prompted re-analysis of the results to better risk stratify and select patients for future interventions. Here we report our analysis of the impact of the novel radiotherapy targeting paradigm on local and distant failure outcomes in 155 patients treated with photon radiotherapy and make suggestions for the targeting paradigms in future clinical trials.

Clinical risk stratification had dominated risk-stratified radiotherapy treatment paradigms up until the discovery of the four biologic subgroups in 2010–2011.[31,32] Risk-stratified radiotherapy consisted of intermediate dose (23.4 Gy) radiotherapy to the craniospinal axis with a subsequent cone down to treat the volumetric extent of the primary site or posterior fossa. High-risk cases were treated to a dose of 36–41.4Gy depending on the extent of disease following by a selective cone down to the IVth ventricle or posterior fossa and areas of known radiographic metastatic disease in the brain and spine ranging from 45–55.8 Gy. Trials as recently as the early 2000s applied a similar approach, but investigators varied in their

Table 2 Primary Site Failure Summary

Project ID	Methylation Subtype	Primary Site at Diagnosis	Histology	Extent of Resection	Failure Type	Imaging Failure Type	CTV Discordant	Dosimetric Type
36	SHH	Vermis	Large cell anaplasia	GTR/NTR	1° Site	Nodular, cystic	No	Central
40	Group 3	IVth Vent	Classic	GTR/NTR	1° Site, PF, Distant	Nodular, subependymal, LMD	No	Central
44	Group 4	IVth Vent	Large cell anaplasia	GTR/NTR	1° Site, PF, Distant	Nodular, subependymal, LMD	No (10.8% outside pCTV)	Central
52	Group 3	IVth Vent	Large cell anaplasia	GTR/NTR	1° Site, PF, Extra-CNS	Nodular	No	Central
62	SHH	Vermis, IVth Vent	Classic	STR	1° Site	Nodular	No	Central
65	Group 4	IVth Vent	Classic	GTR/NTR	1° Site	Nodular	No	Central
75	Group 4	IVth Vent	Classic	GTR/NTR	1° Site	Nodular	Yes (47.3% outside pCTV)	Central
81	SHH	Cerebellar hemisphere	Classic	GTR/NTR	1° Site	Nodular	No	Central
137	SHH	Cerebellar hemisphere	Other	GTR/NTR	1° Site	Nodular, cystic	Yes (67.1% outside pCTV)	In-field (92.3% w/ in 95% IDL)

Each primary site and combined primary site and distant failure case was described according to the relationship of the disease at diagnosis, failure type, imaging failure type, discordance from the delineated CTV volume, and relation to the radiation dosimetry. 1^{o}: Primary site, pCTV: Primary Clinical Target Volume, CTV: Clinical Target Volume, IDL: Isodose Line, w/in: within, PF: Posterior Fossa, IVth: Fourth.

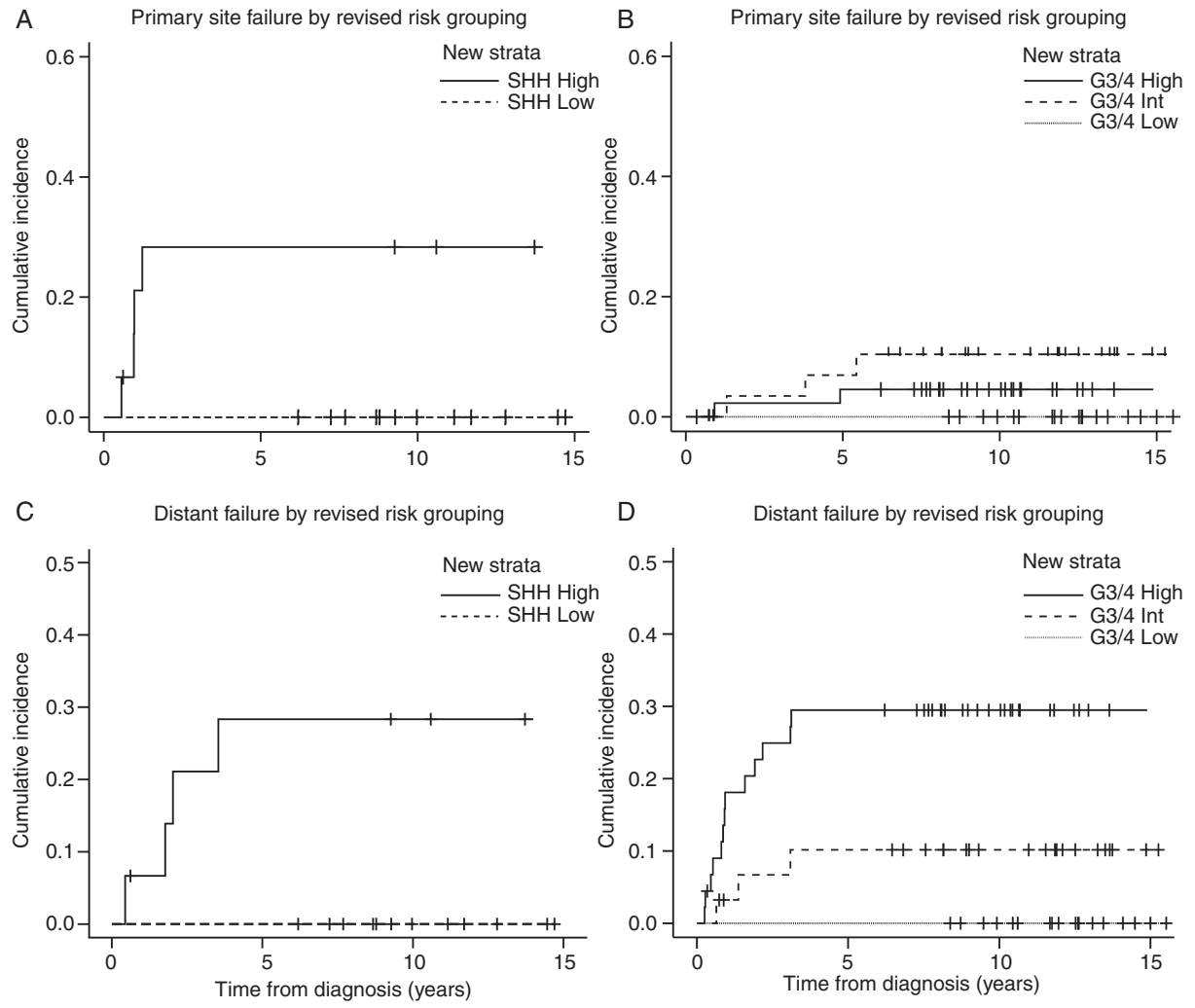

Fig. 3 Primary site and distant failure by revised risk grouping. Cumulative incidence of Primary site failure by the revised risk grouping for SHH (A) and Group 3 and 4 (B). Distant failure by the revised risk grouping for SHH (C) and Group 3 and 4 (D). G3/4: Group 3 and Group 4. Int: intermediate, SHH: sonic hedgehog.

application of a targeting paradigm, which included either the entirety of the posterior fossa or selective volumetric targeting of the IVth ventricle.[33,34] This prompted investigators to consider randomization of both the volumetric targeting of the primary site (all patients) as well as selective dose reduction to the brain and spine axis in standard risk patients (in those 3–7 years of age).[35] A boost to the entirety of the posterior fossa is still often used in high-risk patients, but institutional studies such as SJMB96 and SJMB03 have substantially limited the clinical targeted volume expansion from 2 cm to 1 cm with potential gains in function preservation in the form of reduced hearing loss and reduced cognitive decline.[12,36–38]

The present study highlights sustained disease control in the setting of interval reductions in the integral dose to eloquent structures of the brain, although a substantial influence of methylation subgroup was observed. No WNT patients experienced a clinical relapse. This has been observed by others and has led to two clinical trials (SJMB12[39], ACNS1422[40]) that seek to de-escalate therapy for this subset while maintaining excellent outcomes by reducing the total craniospinal and primary site dose, as well as the systemic therapy exposure in the maintenance phase of therapy.[40] Conversely, a primary site failure rate of 15.2% was observed in the SHH methylation subgroup, although this was most pronounced in the high-risk strata (32% vs. 10%). Other groups have noted adverse outcomes for subsets of SHH patients including those with TP53 alterations[41] although, no one has related this to primary site failure risk. Group 3 patients with standard risk disease were also at increased risk for primary site failure, although this effect was lost in the setting of competing risk for distant failure as observed in Supplementary Figure 6A–D. The revised risk stratification proposed in the full analysis of the results of SJMB03, was also accompanied by a corresponding

increased cumulative incidence of local failure for the SHH high-risk subgroup. While the recently completed ACNS0331 study documented an excess of local failures in SHH patients with posterior fossa radiotherapy (15.8%, 95% CI 2.8–28.7%) relative to those treated with primary site only radiotherapy (0%, 95% CI 0–0%), imbalances in biologically relevant alterations and nuances in risk reporting may confound the interpretation of these results.[14] Concurrent systemic therapy with conventional chemotherapy during radiation therapy has not proven to be useful in this population, although concurrent novel systemic therapies are being explored.[42] The combined results of these studies highlight the need for alternative strategies in M+ SHH high-risk patients, and improved therapies for Group 3 medulloblastoma. It remains unclear if varied radiotherapy fields and dosing,[43] or concurrent systemic therapy[42] are the pathway forward.

While we show excellent disease outcomes with reduced volume primary site radiotherapy, this study was limited by a reduced sample size and lack of randomized cohorts demonstrating expected improvements in functional outcomes. It remains unclear whether we should expect diminishing returns with successive reductions in the extent targeted. Our data highlighting the influence of methylation subgroup and molecular risk stratification raise the potential for differential strategies according to clinical and molecular risk profiles. The latter provides justification for lower cumulative dose and tighter margins for molecularly low-risk tumors. Conversely, molecularly high-risk tumors may require alternative strategies, such as the incorporation of radiation sensitizers, to mitigate against distant failure. These small incremental improvements may potentially lessen the acute and late toxicity burden in childhood medulloblastoma survivors and improve overall disease outcomes.

Conclusion

The differential spatial disease distribution of the varied molecular subgroups of medulloblastoma has a corresponding impact on the pattern of local and distant failure. Revised molecular risk stratification was able to identify subsets of patients with low risk of local and posterior fossa, and metastatic failure which may facilitate innovations in radiotherapy targeting in future studies. Revisiting therapeutic strategies should be considered in molecularly defined subsets where the risk of failure remains high.

Supplementary Material

Supplementary material is available at *Neuro-Oncology* online.

Keywords

Group 3 | Group 4 | medulloblastoma | SHH | WNT

Acknowledgements

The authors would like to thank Keith A. Laycock, PhD, ELS, for scientific editing of the manuscript and Melissa Gargone, MHS, RT(T), CMD, for assistance with radiation dosimetry.

Funding

This work was supported in part by the American Lebanese Syrian Associated Charities (ALSAC), and National Cancer Institute grant P30 CA021765 (St. Jude Cancer Center Support Grant).

Conflicts of interest statement. None, all authors

Authorship statement. Protocol Design: AG, TEM. Wrote, Conceived, and Reviewed the data: JTL, CLT, GWR, BAO. Build the dataset: JTL, CLT, TEM, SS, PT. Analyzed the data: JH, AO-T, JB. Anatomic and Molecular Path review: DWE, PAN, BAO, GWR. Reviewed and approved the manuscript: All authors.

References

1. Ostrom QT, Gittleman H, Xu J, et al. CBTRUS statistical report: primary brain and other central nervous system tumors diagnosed in the United States in 2009–2013. *Neuro Oncol.* 2016;18(suppl_5):v1–v75.
2. Gajjar A, Chintagumpala M, Ashley D, et al. Risk-adapted craniospinal radiotherapy followed by high-dose chemotherapy and stem-cell rescue in children with newly diagnosed medulloblastoma (St Jude Medulloblastoma-96): long-term results from a prospective, multicentre trial. *Lancet Oncol.* 2006;7(10):813–820.
3. Gandola L, Massimino M, Cefalo G, et al. Hyperfractionated accelerated radiotherapy in the Milan strategy for metastatic medulloblastoma. *J Clin Oncol.* 2009;27(4):566–571.
4. Bloom HJ, Wallace EN, Henk JM. The treatment and prognosis of medulloblastoma in children. A study of 82 verified cases. *Am J Roentgenol Radium Ther Nucl Med.* 1969;105(1):43–62.
5. Kann BH, Park HS, Lester-Coll NH, et al. Postoperative radiotherapy patterns of care and survival implications for medulloblastoma in young children. *JAMA Oncol.* 2016;2(12):1574–1581.
6. Silverman CL, Palkes H, Talent B, Kovnar E, Clouse JW, Thomas PR. Late effects of radiotherapy on patients with cerebellar medulloblastoma. *Cancer.* 1984;54(5):825–829.
7. Mulhern RK, Kepner JL, Thomas PR, Armstrong FD, Friedman HS, Kun LE. Neuropsychologic functioning of survivors of childhood medulloblastoma randomized to receive conventional or reduced-dose craniospinal irradiation: a Pediatric Oncology Group study. *J Clin Oncol.* 1998;16(5):1723–1728.
8. Vatner RE, Niemierko A, Misra M, et al. Endocrine deficiency as a function of radiation dose to the hypothalamus and pituitary in pediatric and young adult patients with brain tumors. *J Clin Oncol.* 2018;36(28):2854–2862.

9. Bavle A, Tewari S, Sisson A, Chintagumpala M, Anderson M, Paulino AC. Meta-analysis of the incidence and patterns of second neoplasms after photon craniospinal irradiation in children with medulloblastoma. *Pediatr Blood Cancer.* 2018;65(8):e27095.
10. Fukunaga-Johnson N, Lee JH, Sandler HM, Robertson P, McNeil E, Goldwein JW. Patterns of failure following treatment for medulloblastoma: is it necessary to treat the entire posterior fossa? *Int J Radiat Oncol Biol Phys.* 1998;42(1):143–146.
11. Merchant TE, Happersett L, Finlay JL, Leibel SA. Preliminary results of conformal radiation therapy for medulloblastoma. *Neuro Oncol.* 1999;1(3):177–187.
12. Merchant TE, Kun LE, Krasin MJ, et al. Multi-institution prospective trial of reduced-dose craniospinal irradiation (23.4 Gy) followed by conformal posterior fossa (36 Gy) and primary site irradiation (55.8 Gy) and dose-intensive chemotherapy for average-risk medulloblastoma. *Int J Radiat Oncol Biol Phys.* 2008;70(3):782–787.
13. Hospital SJCsR. Treatment of patients with newly diagnosed medulloblastoma, supratentorial primitive neuroectodermal tumor, or atypical teratoid rhabdoid tumor. 2003. https://ClinicalTrials.gov/show/NCT00085202. Accessed August 12, 2021..
14. Michalski JM, Janss AJ, Vezina LG, et al. Children's oncology group phase III trial of reduced-dose and reduced-volume radiotherapy with chemotherapy for newly diagnosed average-risk medulloblastoma. *J Clin Oncol.* 2021;39(24):2685–2697.
15. Michalski JM, Janss A, Vezina G, et al. Results of COG ACNS0331: A phase III trial of involved-field radiotherapy (IFRT) and low dose craniospinal irradiation (LD-CSI) with chemotherapy in average-risk medulloblastoma: a report from the Children's Oncology Group. *Int J Radiat Oncol, Biol Phy.* 2016; 96(5):937-938.
16. Group CsO, Institute NC. Chemotherapy and radiation therapy in treating young patients with newly diagnosed, previously untreated, high-risk medulloblastoma/PNET. 2007. https://ClinicalTrials.gov/show/NCT00392327. Accessed August 12, 2021.
17. Leary SES, Packer RJ, Li Y, et al. Efficacy of carboplatin and isotretinoin in children with high-risk medulloblastoma: a randomized clinical trial from the Children's Oncology Group. *JAMA Oncol.* 2021;7(9):1313–1321.
18. Northcott PA, Pfister SM, Jones DT. Next-generation (epi)genetic drivers of childhood brain tumours and the outlook for targeted therapies. *Lancet Oncol.* 2015;16(6):e293–e302.
19. Ramaswamy V, Remke M, Bouffet E, et al. Risk stratification of childhood medulloblastoma in the molecular era: the current consensus. *Acta Neuropathol.* 2016;131(6):821–831.
20. Ramaswamy V, Remke M, Bouffet E, et al. Recurrence patterns across medulloblastoma subgroups: an integrated clinical and molecular analysis. *Lancet Oncol.* 2013;14(12):1200–1207.
21. Robinson GW, Rudneva VA, Buchhalter I, et al. Risk-adapted therapy for young children with medulloblastoma (SJYC07): therapeutic and molecular outcomes from a multicentre, phase 2 trial. *Lancet Oncol.* 2018;19(6):768–784.
22. Upadhyaya SA, Robinson GW, Onar-Thomas A, et al. Molecular grouping and outcomes of young children with newly diagnosed ependymoma treated on the multi-institutional SJYC07 trial. *Neuro Oncol.* 2019;21(10):1319–1330.
23. Capper D, Jones DTW, Sill M, et al. DNA methylation-based classification of central nervous system tumours. *Nature.* 2018;555(7697):469–474.
24. Gajjar A, Robinson GW, Smith KS, et al. Outcomes by clinical and molecular features in children with medulloblastoma treated with risk-adapted therapy: results of an international phase III trial (SJMB03). *J Clin Oncol.* 2021;39(7):822–835.
25. Avants BB, Tustison NJ, Song G, Cook PA, Klein A, Gee JC. A reproducible evaluation of ANTs similarity metric performance in brain image registration. *Neuroimage.* 2011;54(3):2033–2044.
26. Zapotocky M, Mata-Mbemba D, Sumerauer D, et al. Differential patterns of metastatic dissemination across medulloblastoma subgroups. *J Neurosurg Pediatr.* 2018;21(2):145–152.
27. Mata-Mbemba D, Zapotocky M, Laughlin S, Taylor MD, Ramaswamy V, Raybaud C. MRI characteristics of primary tumors and metastatic lesions in molecular subgroups of pediatric medulloblastoma: a single-center study. *AJNR Am J Neuroradiol.* 2018;39(5):949–955.
28. Chan JL, Lee SW, Fraass BA, et al. Survival and failure patterns of high-grade gliomas after three-dimensional conformal radiotherapy. *J Clin Oncol.* 2002;20(6):1635–1642.
29. Lucas JT Jr, Cooper DA, Hwang S, et al. Prognostic relevance of treatment failure patterns in pediatric high-grade glioma: is there a role for a revised failure classification system? *Int J Radiat Oncol Biol Phys.* 2017;99(2):450–458.
30. Tinkle CL, Simone B, Chiang J, et al. Defining optimal target volumes of conformal radiation therapy for diffuse intrinsic pontine glioma. *Int J Radiat Oncol Biol Phys.* 2020;106(4):838–847.
31. Gibson P, Tong Y, Robinson G, et al. Subtypes of medulloblastoma have distinct developmental origins. *Nature.* 2010;468(7327):1095–1099.
32. Northcott PA, Korshunov A, Witt H, et al. Medulloblastoma comprises four distinct molecular variants. *J Clin Oncol.* 2011;29(11):1408–1414.
33. Bitsko MJ, Cohen D, Dillon R, Harvey J, Krull K, Klosky JL. Psychosocial late effects in pediatric cancer survivors: a report from the children's oncology group. *Pediatr Blood Cancer.* 2016;63(2):337–343.
34. McClellan W, Fulbright JM, Doolittle GC, et al. A collaborative step-wise process to implementing an innovative clinic for adult survivors of childhood cancer. *J Pediatr Nurs.* 2015;30(5):e147–e155.
35. Michalski J. Comparison of radiation therapy regimens in combination with chemotherapy in treating young patients with newly diagnosed standard-risk medulloblastoma: ClinicalTrials.gov Identifier NCT00085735. 2003. https://clinicaltrials.gov/ct2/show/NCT00085735?cond=00085735&draw=2&rank=12004.
36. Merchant TE, Gould CJ, Xiong X, et al. Early neuro-otologic effects of three-dimensional irradiation in children with primary brain tumors. *Int J Radiat Oncol Biol Phys.* 2004;58(4):1194–1207.
37. Merchant A, Robinson G Proton versus photon radiotherapy for common pediatric brain tumors: comparison of models of dose characteristics and their relationship to cognitive function. *Pediatr Blood Cancer.* 2008;51(1):110–117.
38. Hua C, Bass JK, Khan R, Kun LE, Merchant TE. Hearing loss after radiotherapy for pediatric brain tumors: effect of cochlear dose. *Int J Radiat Oncol Biol Phys.* 2008;72(3):892–899.
39. Gajjar A, Robinson G. A clinical and molecular risk-directed therapy for newly diagnosed medulloblastoma. 2012. https://ClinicalTrials.gov/show/NCT01878617.
40. Gottardo NJ. Reduced craniospinal radiation therapy and chemotherapy in treating younger patients with newly diagnosed WNT-driven medulloblastoma. 2014. https://ClinicalTrials.gov/show/NCT02724579. Accessed August 2021.
41. Zhukova N, Ramaswamy V, Remke M, et al. Subgroup-specific prognostic implications of TP53 mutation in medulloblastoma. *J Clin Oncol.* 2013;31(23):2927–2935.
42. Endersby R, Whitehouse J, Pribnow A, et al. Small-molecule screen reveals synergy of cell cycle checkpoint kinase inhibitors with DNA-damaging chemotherapies in medulloblastoma. *Sci Transl Med.* 2021;13(577):1–16.
43. Tian S, Sudmeier LJ, Zhang C, et al. Reduced-volume tumor-bed boost is not associated with inferior local control and survival outcomes in high-risk medulloblastoma. *Pediatr Blood Cancer.* 2020;67(1):e28027.